

Article

Early Detection of Invasive Exotic Trees Using UAV and Manned Aircraft Multispectral and LiDAR Data

Jonathan P. Dash ^{1,2,*}, Michael S. Watt ³, Thomas S. H. Paul ¹, Justin Morgenroth ²  and Grant D. Pearse ¹

¹ Scion, 49 Sala Street, Private Bag 3020, Rotorua 3010, New Zealand

² New Zealand School of Forestry, University of Canterbury, Christchurch 8140, New Zealand

³ Scion, P.O. Box 29237, Fendalton, Christchurch 8041, New Zealand

* Correspondence: jonathan.dash@scionresearch.com

Received: 5 June 2019 ; Accepted: 23 July 2019 ; Published: 2 August 2019



Abstract: Exotic conifers can provide significant ecosystem services, but in some environments, they have become invasive and threaten indigenous ecosystems. In New Zealand, this phenomenon is of considerable concern as the area occupied by invasive exotic trees is large and increasing rapidly. Remote sensing methods offer a potential means of identifying and monitoring land infested by these trees, enabling managers to efficiently allocate resources for their control. In this study, we sought to develop methods for remote detection of exotic invasive trees, namely *Pinus sylvestris* and *P. ponderosa*. Critically, the study aimed to detect these species prior to the onset of maturity and coning as this is important for preventing further spread. In the study environment in New Zealand’s South Island, these species reach maturity and begin bearing cones at a young age. As such, detection of these smaller individuals requires specialist methods and very high-resolution remote sensing data. We examined the efficacy of classifiers developed using two machine learning algorithms with multispectral and laser scanning data collected from two platforms—manned aircraft and unmanned aerial vehicles (UAV). The study focused on a localized conifer invasion originating from a multi-species pine shelter belt in a grassland environment. This environment provided a useful means of defining the detection thresholds of the methods and technologies employed. An extensive field dataset including over 17,000 trees (height range = 1 cm to 476 cm) was used as an independent validation dataset for the detection methods developed. We found that data from both platforms and using both logistic regression and random forests for classification provided highly accurate ($\kappa < 0.996$) detection of invasive conifers. Our analysis showed that the data from both UAV and manned aircraft was useful for detecting trees down to 1 m in height and therefore shorter than 99.3% of the coning individuals in the study dataset. We also explored the relative contribution of both multispectral and airborne laser scanning (ALS) data in the detection of invasive trees through fitting classification models with different combinations of predictors and found that the most useful models included data from both sensors. However, the combination of ALS and multispectral data did not significantly improve classification accuracy. We believe that this was due to the simplistic vegetation and terrain structure in the study site that resulted in uncomplicated separability of invasive conifers from other vegetation. This study provides valuable new knowledge of the efficacy of detecting invasive conifers prior to the onset of coning using high-resolution data from UAV and manned aircraft. This will be an important tool in managing the spread of these important invasive plants.

Keywords: bio-security; LiDAR; invasive plants; random forest; logistic regression; drones; RPAS; invasion monitoring; invasive alien plants; multispectral

1. Introduction

Conifers are among the most economically important tree species on Earth, forming the basis of major forest industries and contributing substantially to the global annual timber yield [1]. Exotic conifer plantations form the cornerstone of the plantation forestry sector in many Southern hemisphere countries. These forests provide significant economic [2,3], social [4], and ecological benefits [5,6] and contribute significantly to global carbon sequestration [7,8]. Furthermore, these forests are critical in supplying the increasing fiber demands of the Earth's growing population [9]. The values provided by plantation forests in many countries are widely recognized, but when planted in inappropriate areas, this valuable land use can have deleterious effects at a local scale. Many conifer species have evolved to exploit a variety of ecological niches which makes them highly suited as fast-growing plantation species. Unfortunately, the same traits also make them highly invasive in some environments [1] as they may out-compete indigenous vegetation. The prevalence of invasions by non-native invasive plants has considerable consequences in many environments and is a significant, and increasingly common, challenge for land managers [10,11]. This is particularly true in mountainous areas where increasing levels of anthropogenic disturbance coupled with a changing climate are expected to trigger an increase in the abundance of invasive plants, and upward expansion of exotic invasive species in vulnerable mountainous regions [12]. Historically, trees did not feature prominently in global lists of important invasive plants [10], but more recently the invasive and unfavorable nature of many tree species has been recognized [13–15]. Now, many tree species are included in databases of the most widespread and damaging plants [14].

In New Zealand, a few conifer species constitute the vast majority of the plantation forestry industry contributing significantly to the country's economic and social well-being. The forestry sector contributes almost NZ\$ 5 billion in export earnings to the economy per year and directly employs some 18,000 people [16]. Despite these benefits, several exotic conifer species have become invasive and are invading natural, and semi-natural, grass and scrubland habitats [17]. These invasions have ecological, economic, and cultural implications within many ecosystems [18]. Exotic conifers have invaded large areas in both North and South Islands primarily in grassland and shrubland areas [19,20]. The area affected by invasive conifers is estimated to be 1,700,000 ha, an area approximately equivalent to the national plantation estate, and this area is thought to be increasing at 5–6% per year [21].

The negative implications of this infestation are considerable, and to control, or at least slow, their spread, detection and eradication methods are required. A range of chemical and physical control methods are available, but to be effective these require accurate detection methods so that they can be targeted efficiently. For control efforts, identifying juvenile trees before they reach maturity is of considerable importance to prevent further spread. This complicates detection solutions because the ease of detection is dependent on the density of the infestation, size of the individuals present [22], and the complexity of the terrain and vegetation structure in the area of interest [23]. In New Zealand, current surveillance and monitoring methods rely on manual conifer detection across larger areas using helicopter-based surveys by skilled operators [24], ground surveys in very small areas, or combinations of both [25]. Detection success using current approaches is highly variable, and detailed surveillance across national or regional scales is not feasible due to high costs and resource limitations. The information void caused by a lack of an effective method for detection of invasive conifers is a major hindrance to the development of effective control procedures.

Remote sensing potentially provides a means for accurate invasive conifer detection over large areas with varied terrain and vegetation types. Automated and semi-automated techniques have been widely used to detect and monitor invasive plants in numerous environments [26–29]. However, research into the detection and monitoring of invasive conifers is limited. Recent research has developed a method for invasive conifer detection by classifying airborne laser scanning (ALS) returns from invasive conifers by combining ALS data with aerial imagery [22]. However, these methods have only been tested in a single vulnerable habitat type and for detection of mature trees. Further research is required to test methods in other settings using data from alternative platforms, and to extend the

methods to juvenile trees. High-resolution aerial imagery has recently been used to accurately classify invasive plants including mature conifers in Chile [30] and New Zealand [31]. However, no research has addressed the issue of identifying invasive trees prior to, or immediately after, the onset of coning when the spread may be controlled more efficiently. Other relevant research comes from the boundary of the boreal and Arctic ecotones [32–37] where there is considerable interest in monitoring changes in the tree line that are associated with climate change. However, there are considerable differences in environmental conditions between Scandinavia and New Zealand and so specialized techniques must be developed in both areas. In particular, the Scandinavian research frequently targets detection of all trees in the area of interest as the presence of any trees represents a shift in vegetation type. This is unsuitable in New Zealand as detection techniques must differentiate invasive conifers from non-target trees and shrubs in many environments.

A range of active and passive remote sensing technologies have been shown to be useful for the detection and monitoring of invasive exotic, or pioneer, trees in studies around the world. These studies include the use of ALS data either alone [36] or in combination with spectral data [22,33,38,39]. The use of passive remote airborne or space-borne sensors for monitoring plant invasions is much more common [29,40–43]. The efficacy of these approaches is dependent on the selection of the appropriate sensor and platform that can provide imagery at the appropriate spatial, spectral, and temporal resolution to separate the target plant species from its surroundings. Data fusion refers to the integration of remotely sensed datasets to provide insight into the properties of target objects. In a forest description context, these fused datasets frequently have greater predictive power than their constituents [44]. Several studies have employed data fusion for detection and monitoring of invasive plants to enhance the separability of the target organism in its environment. Combining the structural information from ALS data with spectral data from hyperspectral or multispectral imagery has proved to be particularly useful for differentiating target organisms from non-target objects [22,45–47]. The constituent datasets can either be sourced from the same or separate platforms depending on the study design.

The resolution of imagery used for invasive plant detection ranges from low spatial resolution datasets such as MODIS [48] which have limited utility for invasive plant detection to studies using ultra-high-resolution imagery collected from unmanned aerial vehicles (UAV)s [49–52]. A range of satellite products have been used in studies monitoring exotic plant invasions. These range from studies using moderate resolution sensors such as Landsat (spatial resolution = 30 m) [53–55], to higher spatial resolution sensors such as WorldView 2 (spatial resolution = 0.5 m) [56] and Pleiades 1A (spatial resolution = 0.5 m) [57,58]. Higher resolution imagery collected from conventional manned aircraft has been widely used for invasive plant detection. These studies include a range of sensors including multispectral [59–61] and hyperspectral imagery [62–68] but none of these studies have focused on small juvenile plants.

In more recent years, the emergence of ultra-high-resolution data collected from UAVs, and their application to forest monitoring [69,70], has allowed the spatial resolution and threshold size of targeted invasive plants to be reduced. This potentially enables the detection and monitoring of earlier invasion stages and smaller plants to be detected. These platforms and associated miniaturized sensors have also significantly reduced the cost and improved the flexibility of acquisition of detailed remotely sensed data [71]. Studies using UAVs for detection of invasive plants have emerged in recent years from Africa [51], North America [50,72], South America [30,73], and Europe [52,74–76] with encouraging initial results.

The earliest UAV-based studies were undertaken in an agricultural setting and made use of computer vision to identify weeds [77]. Significant knowledge gaps remain, and further methodological research is required to develop the promise of these early studies as technical constraints are increasingly cited as a major factor limiting the success of remote sensing assisted invasive plant management [78]. Furthermore, no studies have sought to develop UAVs specifically as a tool for the early detection of plant invasions [79], and this capability is critical to assist with the

eradication of invasive conifers from protected areas. Despite the significant body of research into the detection and monitoring of invasive plants, we are unaware of any studies that focus on detection of invasive trees during the juvenile phase of development either before or immediately after the onset of reproductive maturity. This is critically important and represents a significant challenge as coning can occur very early for some species in many environments, meaning that target objects can be very small. Furthermore, no research has directly compared the efficacy of combinations of spectral and ALS datasets obtained from UAV (UAV-LS) and manned airborne platforms.

In this research, we seek to define the detection threshold and to characterize errors for invasive tree detection in a relatively simplistic grass and shrubland setting. We also examine the efficacy of two different classification approaches in this context and compare the predictive power of combined datasets, containing information from both multispectral and laser scanning, with data provided by single sensors.

2. Materials and Methods

A schematic diagram illustrating the methods used in this paper is included below (Figure 1). Briefly, two sets of remotely sensed data collected from a UAV and manned aircraft platform were used alongside a manually digitized training data set defined in a Geographical Information System (GIS) to fit supervised classification models using either random forests (RF) or logistic regression (LR). For each classifier a total of 11 models were generated using UAV data and 9 models were constructed using manned aircraft data, as the latter have one less band than the UAV data, using a combination of spectral, ALS data, and a combination of both data sources (Table 1). Using this approach, a total of 40 models were created. A k-fold cross-validation [77,80,81] was used to assess model precision based on the accuracy statistics described below.

Table 1. Summary of the all models developed for selection of the best performing model of each class with model performance assessed based on cross-validation statistics from the model fitting dataset.

Model ID	Features	Model Class
1	Blue, Green, Red, Near-infrared, CHM height	Spectral + ALS
2	Blue, Green, Red, Red edge, Near-infrared, CHM height	Spectral + ALS
3	CHM height	ALS
4	Blue, Green, Red, Red edge, Near-infrared	Spectral
5	Blue, Green, Red, Near-infrared	Spectral
6	Blue, Green, Red,	Spectral
7	Red	Spectral
8	Green	Spectral
9	Blue	Spectral
10	Near-infrared	Spectral
11	Red Edge	Spectral

The best performing models were then selected from 12 categories that included the factorial combination of the two platforms, two classifiers and three classes of data (spectral, ALS, spectral and ALS). These 12 models were then used to make predictions about the presence or absence of invasive exotic conifers across the area of interest. These surfaces were then intersected with a completely independent validation dataset sampled from an extensive field data collected within the area of interest to calculate error statistics and to investigate the relationship between detection accuracy and tree size.

2.1. Study Site

The study site is in the Mackenzie Basin, South Canterbury, South Island of New Zealand. Topographically the area was strongly influenced by its glacial history with in-filled and now wide expanding river terraces and glacially formed rounded hills surrounded by high altitude mountain

ranges. The Mackenzie Basin lies between 600–1100 m above sea level (a.s.l.) with higher slopes and hilltops also present near Lake Pukaki. The climate can be characterized as continental with dry hot summers and cold winters. The area has been dominated by native (and more recently a growing proportion of exotic) grassland species for at least the last 500 years and has been subjected to 200 years of pastoral management of varying intensities. This management combined with frequent burning, overgrazing, and incursions of rabbit outbreaks has resulted in a high level of degradation of the natural short and tall tussock grasslands and herb and shrub communities.

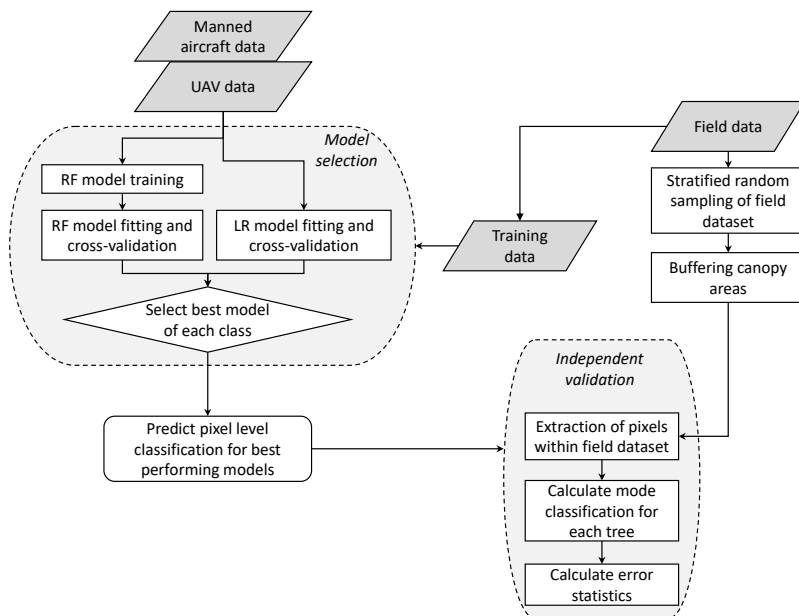


Figure 1. A schematic overview of the methodology used in this research.

In this area, sources for exotic conifers have been historic plantings of shelter belts and woodlots for soil conservation, shelter, scenic, and recreational purposes across the basin. Some commercial plantings were also established over time to create a timber resource. Exotic conifer species originating from these plantings have now become invasive over thousands of hectares and the initial low densities of scattered trees are now expanding to become grassy woodlands, and even dense forested stands in some areas. The major species that have spread across most of the basin and have been controlled, but not eradicated, include *Pinus contorta* Douglas, *Pinus nigra* Arnold, *Pinus sylvestris* L., *Pinus ponderosa* Douglas, *Larix decidua* Mill., and *Pseudotsuga menziesii* (Mirb.) Franco.

The core study area used to develop and test detection methods encompassed 22.4 ha in the immediate vicinity of a shelter belt planted with a mixture of *P. sylvestris*, *P. ponderosa* and a small number of *P. nigra*. The study site is 804 m asl and is located around 11 km west of the township of Lake Tekapo (Latitude = 43° 59' 02.2985 S, Longitude = 170° 20' 22.43 E) (Figure 2). This site was selected because it represented a first-order invasion event of significantly problematic invasive conifer species within this region and provided a suitable testing ground for method development. The flat to rolling terrain of the study site represents mostly short tussock grassland, the common vegetation type in the lower parts of the Mackenzie Basin. Most common native and exotic grasses are short stature tussock species and exotic grasses such as. Shrubs are mostly in the prostrate growth form, are also present and distributed sporadically throughout the area. The herbaceous component of the vegetation is dominated by exotic *Hieracium* species.

2.2. Field Data

Field data were collected at the study site during an extended field campaign between 15th November 2017 and 10th December 2018. The field campaign was interrupted several times

by adverse weather events. The objective of the field survey was to provide a total census of a first-order invasion event from a *P. sylvestris* and *P. ponderosa* shelter belt in an open grassland environment. Aerial imagery was used to manually identify the approximate spread fan of the invasion front. This was used to define the boundary for an on-ground comprehensive search of the study area. Excluding the shelter belt all exotic conifers in the area of interest were identified down to a minimum tree height of 0.05 m. The location of each individual was recorded using a Trimble Geo 7X GNSS receiver. At least 100 epochs were recorded for each individual and points were then post processed using a local base station network maintained by Land Information New Zealand (LINZ). In addition to the tree location, detailed information on the properties of each tree were measured. Total tree height was measured using a height pole and crown width was estimated based on two perpendicular tape measurements including the widest point of the crown. In addition to the species, coning (present/absent), and health status (alive/dead) of all trees was recorded. The age of a subset of trees was estimated using the number of branch whorls and the ground cover (bare ground/tussock/exotic grass cover) in which younger trees have established (<1 m ht) was recorded. This field data collection was used to provide ground-truth data suitable for developing and validating methods for tree detection of all exotic conifers in the area of interest based on the remotely sensed data available.

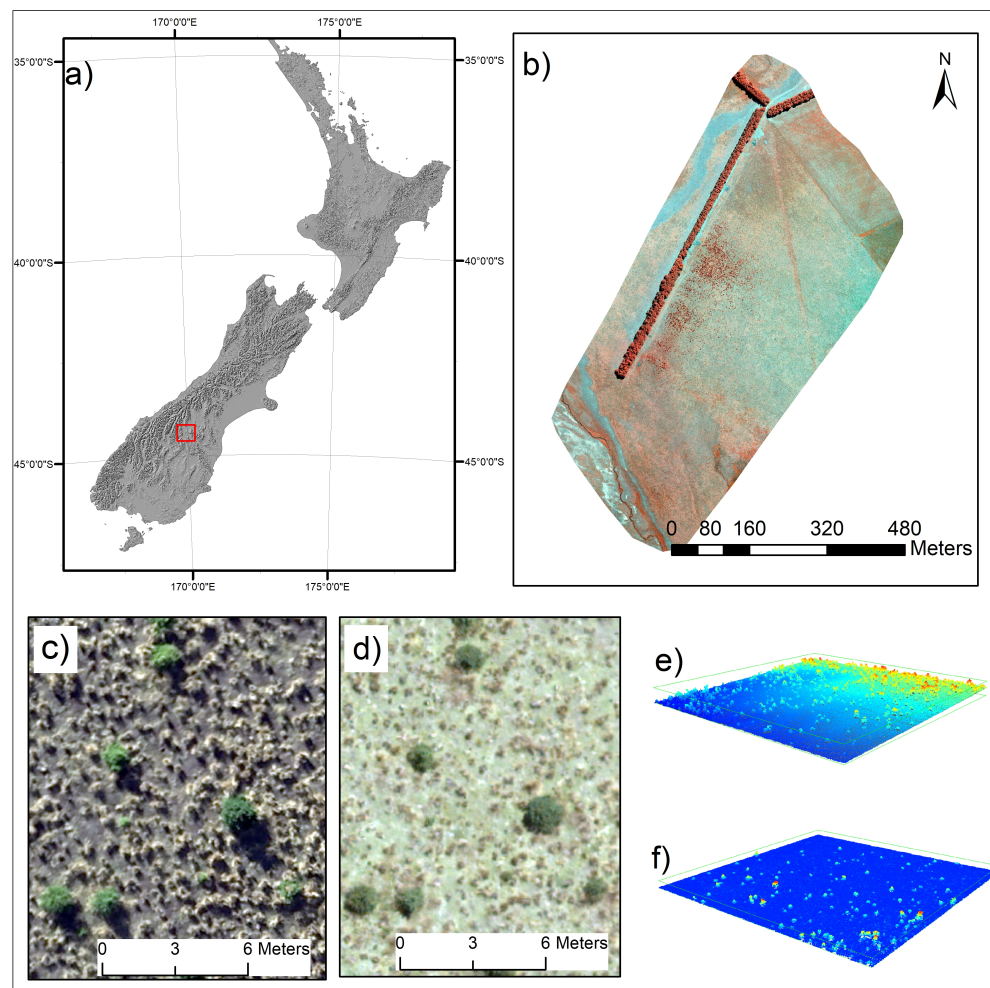


Figure 2. (a) The location of the Mackenzie Basin within New Zealand, outlined in red over a shaded relief map, (b) an overview of the site, (c) a close up of the UAV imagery used in the study, (d) a close up of the manned aircraft imagery used in the study, (e) a part of the UAV-LS point cloud, and (f) a part of the ALS point cloud collected from the manned aircraft.

2.3. Remotely Sensed Data

Remotely sensed data were collected from the study site using both UAV and manned platforms. Wall to wall coverage of point clouds derived from laser scanning and orthomosaics of multispectral imagery was acquired from both platforms for the study area.

2.3.1. Manned Aircraft Data

Both imagery and ALS data were collected simultaneously on 29th January 2018. Imagery was collected using a Leica RCD30 camera with an 80 mm lens (Field of view 60°) and laser scanning was carried out using a Leica ALS60 scanning system. Data were collected from onboard a Remi Cessna 337 Skymaster across the study site at a flying height of 800 m above ground level. The cruise speed was 120 knots and terrain following was undertaken manually by the pilot. The resultant imagery had a ground sampling distance (GSD) of 4 cm. The 80 MP medium format camera used provided high-resolution four band multispectral imagery with radiance recorded in the blue (450–485 nm), green (500–565 nm), red (625–680 nm), and near-infrared (780–880 nm) bands. The laser scanning system was capable of recording up to 5 returns per pulse. Data were collected with a pulse repetition frequency of 120 kHz and a mean swath overlap of 45% which resulted in a point cloud dataset with a mean point density of 8.28 pts/m² (standard deviation = 1.81 pts/m²) and a mean ground spacing of 0.35 m (Table 2). A series of ground control points were established by the provider and used to orthorectify both the aerial imagery and the point cloud data. This resulted in a mean reported accuracy of 0.1 m in both the horizontal and the vertical dimensions with a 90% confidence interval.

Initial point cloud processing was carried out using the Terrasolid software (Terrasolid Oy, Espoo, Finland). This included tiling, classification of noise points, and ground classification. Subsequent processing was carried out in the LAStools software suite or and the lidR package [82] within the R statistical software package [83].

2.3.2. UAV Data

UAV laser scanning data were acquired on the 6th May 2018 using a Velodyne HDL-32E (Velodyne, San Jose, CA, USA) scanner embedded in a RouteScene ‘LidarPod’ laser scanning system (Mapix Technologies Ltd., Edinburgh, UK). The laser scanner was mounted on a DJI Matrice 600 piloted octocopter platform (DJI Ltd., Shenzen, China), in total 9 flights were required to cover the entire study area. The Velodyne HDL-32E laser scanner has a rotating array of 32 lasers, providing a maximum potential ‘scan angle’ of 180 degrees from the Routescene system. Only the inner lasers are equiangular and returns acquired with a high off-nadir angle can induce substantial artefacts and noise in the point cloud data when acquired from a UAV. To minimize these effects, only data from the inner-most lasers (± 8 degrees off nadir) were retained and a sector reduction filter was applied to limit the effective scan angle to ± 25 degrees. Flight line matching, ground classification, noise removal and the identification of overlap points were carried out in Terrasolid. Subsequently, points classified as overlap were removed to ensure a more even density over the entire study area. A flying altitude of approximately 60 m above the local terrain and a flight speed of 6 m per second was used. The flight plan ensured that there was significant side overlap to remove the possibility of data voids. All flight maneuvers and altitude adjustments were made outside of the area of interest to avoid the possibility of flight artefacts in the dataset. The laser scanner was only capable of recording a single return and produced a pulse density of 121 pls/m² and a mean ground pulse spacing of 0.09 m (Table 2).

Multispectral imagery was acquired on the 9th May 2018 from the same UAV in a separate campaign that included 4 flights. A Sentera Multispectral Double 4K camera (Sentera, Minneapolis, MN, USA) was used for UAV-borne multispectral data collection. This sensor provides imagery in the blue (416–476 nm), green (525–570 nm), red (615–695 nm), red edge (700–740 nm), and near-infrared (830–850 nm). Imagery was captured from an altitude of 80 m agl and flight settings ensured a front

and side overlap of 70% and 80% respectively. The resulting geo-referenced mosaic dataset had a GSD of 2.5 cm.

Table 2. Summary of the ALS and UAV-LS datasets used in this analysis.

Platform	Sensor	Point Density	Point Spacing	Altitude (m)	Returns
UAV	Velodyne HDL32e	121	0.09	60	1
Manned	Leica ALS60	8.28	0.35	800	5

2.3.3. Data Processing

The UAV-LS and ALS datasets used to generate canopy height models (CHM) covering the study area. Several approaches to CHM generation were trialed and were assessed visually to identify the dataset that contained the most accurate representation of the conifer invasion spread. A CHM was generated from both datasets and was used to produce rasters characterizing vegetation height across the study area. The CHM resolution was chosen to reflect the approximate footprint size of each dataset (UAV-LS = 0.1 m, ALS = 0.3 m).

The CHM rasters were co-registered with the multispectral imagery using features that could be manually identified in both the CHM and in the imagery using the geo-rectification tool in the ArcGIS software suite (Esri, Redlands, USA). Using the manually identified tie points, rectification was carried out using a first-order polynomial (affine) transformation to shift, scale, and rotate the raster datasets. The resulting RMSE was 42 and 35 cm for the manned aircraft and UAV imagery respectively using the 40 link tie points identified independently for each set of rasters. The CHM rasters were resampled to the same resolution as the respective multispectral imagery collected from each platform using the gdalwarp function of the Geospatial Data Abstraction Library [84] (GDAL version 2.2.4).

2.4. Supervised Classification

Supervised pixel-based classification was used to develop models for detection of invasive conifers. A training dataset was produced through careful digitization of 50 conifer canopies within a GIS and 50 areas of background vegetation. Areas that were very heavily shaded were excluded from the training dataset as this has been shown to improve classification results using UAV imagery [30]. The spatial data were exported from the GIS and loaded into R [83] where they were used to extract classified pixels coincident with the selected areas. Therefore, a training dataset containing 2,057,915 pixels including ground-truth labels indicating conifer/background and spectral data and CHM elevation data derived from the ALS or UAV-LS as the candidate predictive variables. The statistical learning method RF [85] and LR method using a generalized linear model (GLM) were used. For the RF algorithm, model training was carried out using the Caret package [86] using ten-fold cross-validation with three repeats. Classifiers were developed using the R packages ranger [87] for RF, and glm [83] for LR. In total, 42 models were developed; these included either spectral data only, spectral data and ALS, or ALS data only and separate models were developed for each platform and model class (RF or LR). The best models of each class for each platform and model type were identified, using the validation statistics calculated for accuracy assessment. These classifiers were used to predict the presence of invasive across the study site.

2.5. Accuracy Assessment

The predictions from the best performing model of each class identified in Table 1 were used for independent validation of model accuracy. An independent validation dataset was generated using stratified random sampling of individual conifers from the field data. Stratification was based on tree height, using classes with 0.25 m increments, with the intention of ensuring that trees of all sizes were included in the validation dataset. It was intended that this would provide insight into the relationship between tree size and classifier performance. Ten individuals were randomly selected

from within each stratum. Once identified, the canopies of the invasive conifers in the validation dataset were represented as circular cross-sectional areas—with the diameter of each extracted from the field measured canopy widths. The cross-sectional canopy areas were used to extract pixels from the classification results from the selected models that were coincident with the field measured tree canopies. The mode of the classified pixels within a field measured tree canopy was used to define the overall classification value for a subject tree and statistics were calculated at the tree level. The sampling process was iterated five times to allow the sample to stabilize and reduce the possibility of sample artefacts affecting the interpretation of the results. The independent validation dataset was completed by randomly selecting 800 m² square areas of the surrounding land that the field data and imagery indicated were free from invasive conifers.

Accuracy statistics were calculated and used during both the model selection and independent validation. The accuracy of the supervised classification model was assessed through a repeated cross-validation of the training dataset with five folds and ten repeats. Simple accuracy, Cohen's Kappa statistics [88], area under the receiver operator curve (AUC), and F measure based on the cross-validation were calculated and used to assess classification accuracy. Similarly, these statistics were also calculated at the individual tree level during the independent validation exercise. Furthermore, the sensitivity and specificity of each classification model was calculated to provide further insight into classifier performance. Sensitivity was calculated as the count of true positive classifications divided by the sum of true positives and false negatives. Specificity was calculated as the count of true negatives divided by the sum of true negatives and false positives [86].

3. Results

3.1. Field Data

In total 17,514 invasive conifers were identified and measured in the study site during the field campaign. Of this sample, 99% were either *P. sylvestris* (60%) or *P. ponderosa* (39%), these being the two species that comprise the shelterbelt in the study area. A small minority (3.55%) of the trees were observed to be dead at the time of assessment and these were removed from the subsequent independent validation. The field data showed that the *P. sylvestris* trees within the study area were markedly taller and had larger crowns than the *P. ponderosa* (Table 3). Following differential correction, the mean reported precision of the field recorded tree locations was 0.08 m. This level of accuracy is considerably smaller than the crown width of the majority subject trees and should not significantly affect the results reported here. Plotting the tree locations showed that the two species were not uniformly intermingled but exhibited species clustering probably associated with the availability of seed source, timing of seed release, and local soil and terrain conditions. Only the *P. sylvestris* was found to be coning in the field dataset (Figure 3b). In total, 657 trees were found to be coning. These trees had an average height of 2.43 m and an average crown diameter of 1.58 m. Notably, the smallest tree found to be coning was only 0.84 m tall (crown diameter of 0.37 m) (Figure 3). However, in total, only 5 coning trees (0.07%) were found to be under 1 m tall.

Table 3. Summary of the field data collected and used in the independent validation dataset. Values in brackets show the range of the measured tree heights and crown widths.

Species	n	Mean Height (cm)	Mean Crown Width (cm)
<i>P. ponderosa</i>	6621	40.90 (2–369)	46.59 (1–228)
<i>P. sylvestris</i>	10,032	95.76 (1–476)	102.60 (1–325)

In addition to the spatial distribution and species composition, the size of the trees and the density of the invasion are also of critical importance. The interaction of density with tree size affects both the difficulty of detection and the strategy that might be deployed for control and eradication. Based on the field dataset the density of invasive conifers across the study site was calculated (Figure 3). This

analysis revealed that the density of invasive conifers was highest closest to the shelter belt and decreased further away from where only small groups or individuals were present.

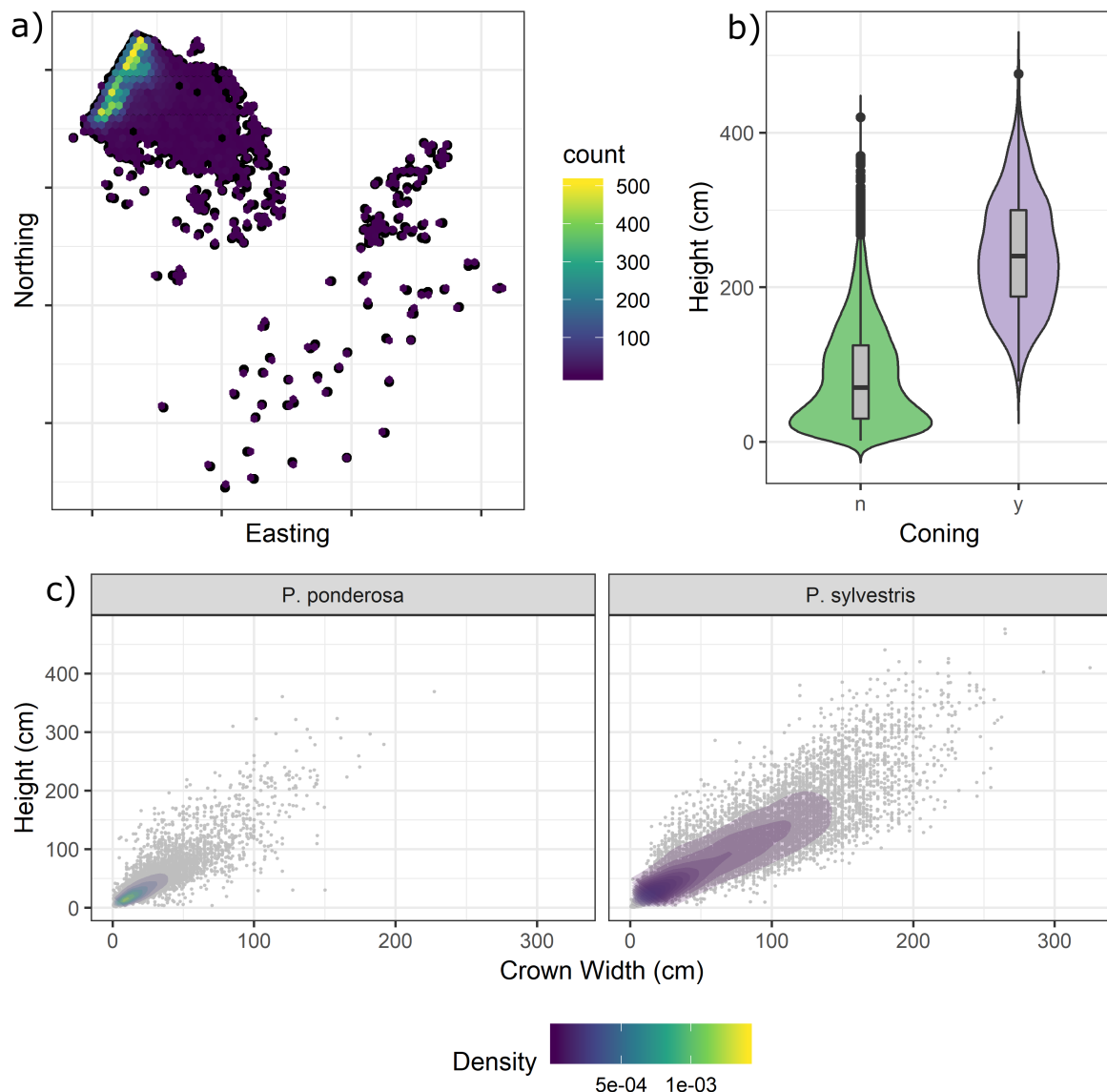


Figure 3. (a) A hexplot showing the spatial distribution and density of invasive conifers in the field dataset, (b) a violin and box plot showing the height distribution of non-coning (n) and coning (y) trees in the field dataset, and (c) the relationship between height and crown width for *P. ponderosa* and *P. sylvestris*.

3.2. Training Data

Two separate datasets were produced for training the supervised classifiers from the remotely sensed data. Graphical analysis of the training datasets provided insight into their properties (Figure 4). This analysis showed that there were significant differences between datasets acquired from the UAV and manned aircraft. It was particularly evident that the tussock areas in the manned aircraft training data were considerably brighter than their equivalent areas in the UAV training dataset. This is likely due to differences between sensors and variation in the atmospheric and solar conditions in between the two acquisitions. As a result of this, the invasive conifer pixels were considerably more distinct from their surroundings in the manned aircraft data than in the UAV imagery data in terms of the

spectral bands available. However, it is clear from Figure 4 that there was a substantial difference in the values in the red edge band between areas containing invasive conifers and those that did not.

For both datasets, the structural properties of the invasive conifers varied greatly from their surroundings as the elevation of returns originating in the invasive conifers was usually considerably greater than zero (Figure 4). The median and upper quartile of the elevation of returns from invasive conifers were very similar in datasets from both platforms. The lower quartile of the elevation distribution was considerably lower for the manned aircraft dataset than for the UAV data.

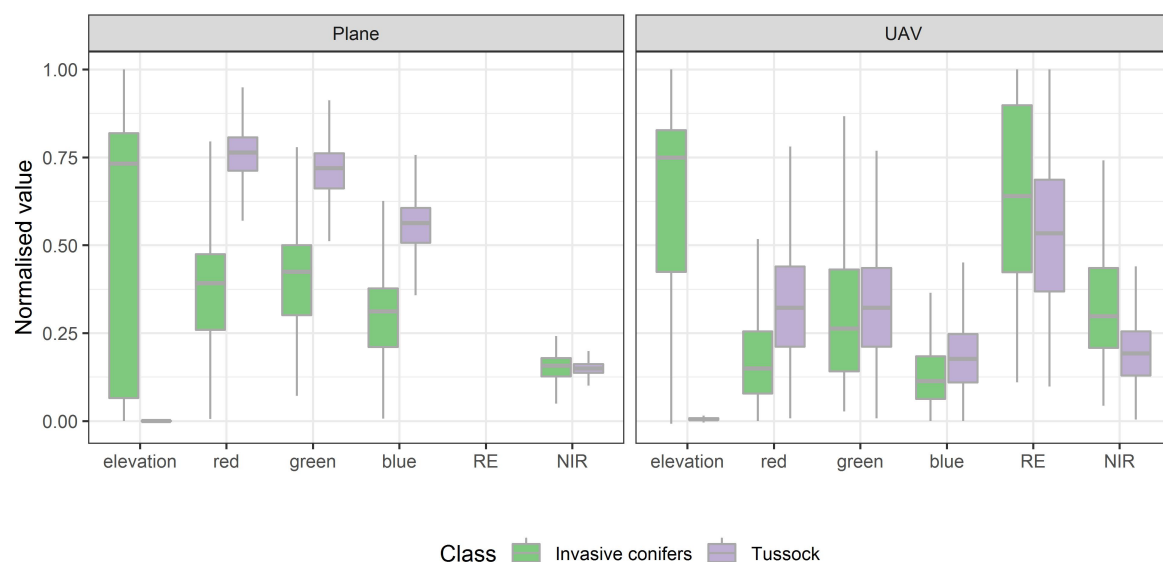


Figure 4. Box and whisker plots of the spectral and structural properties of the training dataset for the manned aircraft (Plane) and UAV datasets.

3.3. Model Development

The classification accuracy results extracted from the cross-validation process during model development and model selection are shown in Table 4 and Figure 5. Models developed using ALS and all spectral data (models 1 and 2), all available spectral data (models 4 and 5), or only ALS (model 3) were exceptionally accurate and had kappa values greater than 0.96 for all four combinations of classifier and platform (Figure 5). Similarly, there was very little difference between the classifiers and platform using models with four combinations of spectral bands and these two models (models 4, 5) had very high kappa values (>0.996) that were very similar to the first three models. The models developed with red, green, and blue bands (model 6) were very accurate but the classification accuracy was slightly higher for these models using data derived from the UAV (mean kappa = 0.990) than the data from the manned aircraft (mean kappa = 0.942).

Using data from the manned aircraft, the accuracy of the models that used only a single spectral band (models 7–11) were very similar between the two classifiers (Figure 6). Mean kappa values for these models were respectively, 0.628, 0.617 and 0.406 for models with red, green, and blue bands. For both classifiers the model with the near-infrared band was the least accurate, but classification accuracy for this model was higher for the RF model (kappa = 0.366) than for the model created using LR (kappa = 0.202). The red edge band was only available using UAV-borne sensor and was more accurate (kappa = 0.732) for the LR than for the RF model (kappa = 0.272).

In contrast to the data from the manned aircraft, classification accuracy for single band models developed from the UAV were, with the exception of the model with the near infra-red band, markedly lower (Figure 5). LR generally outperformed RF with these single band models (Figure 5). Kappa values for this classifier were respectively 0.637, 0.794, 0.403 and 0.202 for models 6–10, which included the single respective bands of red, green, blue, and NIR bands.

Based on these results, the best performing models for each class (spectral + ALS, spectral, and ALS) were identified and used in subsequent independent validation of classifier performance and mapping of invasive exotic conifers across the study site. The best performing models of the spectral + ALS class and the spectral class contained all available spectral predictors (R, G, B, NIR for the manned aircraft and R, G, B, NIR, and red edge for the UAV).

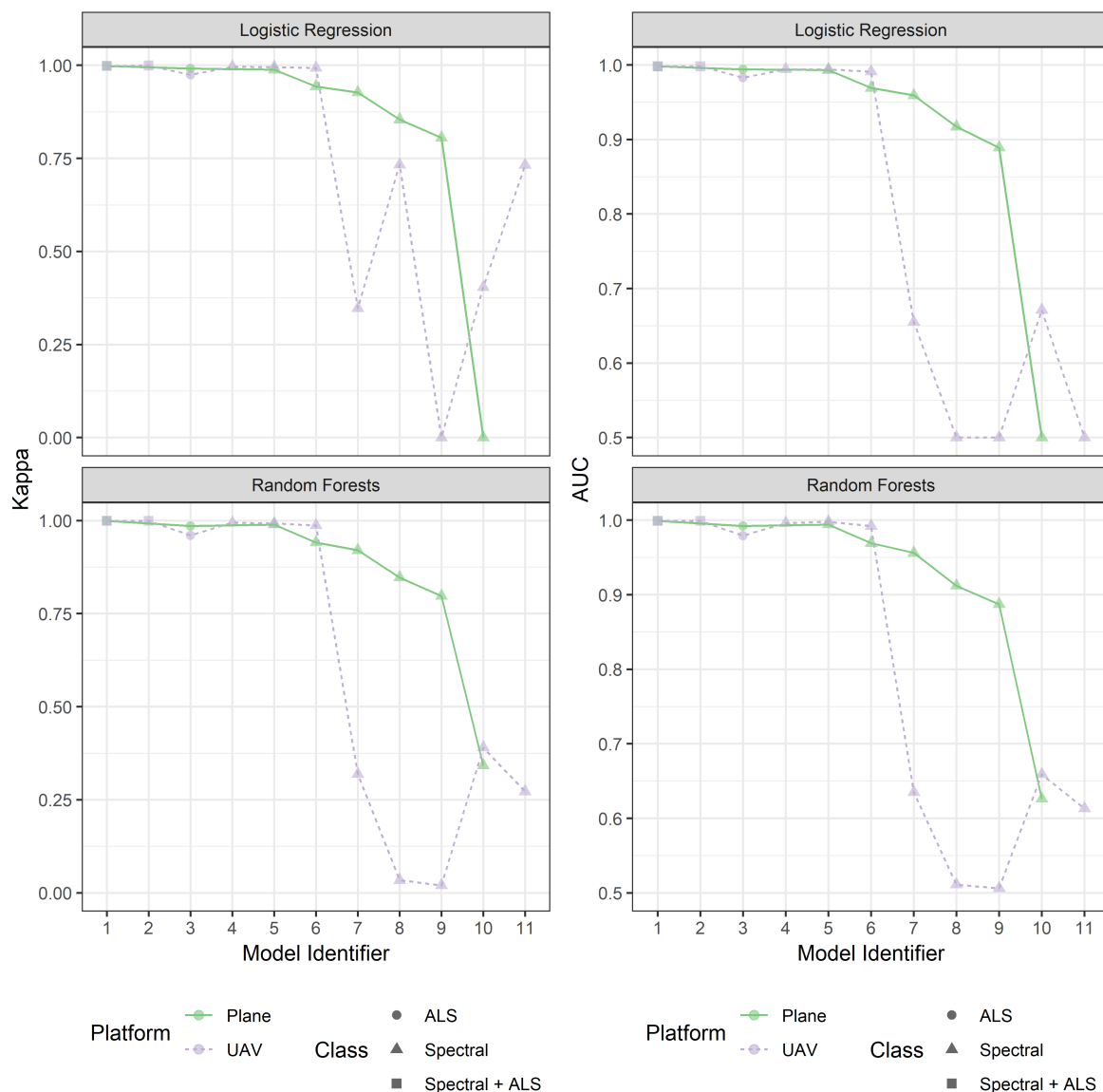


Figure 5. Kappa values extracted from the cross-validation results during model development. Each datum represents the kappa value from cross-validation for a single model. The model identifiers as shown in Table 1 are shown along the X axis and shape of each datum represents the class of model represented. Please note that models 2 and 11 could only be developed using UAV data as these included the red edge band.

3.4. Independent Validation

Rasters detailing the pixel-wise predictions from the best performing model for each model type were generated for the study area (Table 4). Only the best performing models of each class were used for the independent validation (Table 4). The independent validation showed that overall the three best performing models used the UAV data for classification. The best performing model was a LR model using all available spectral predictors ($\kappa = 0.709$), followed by a RF model using the same

spectral predictors ($\kappa = 0.633$), and the RF model using both spectral and UAV-LS predictors ($\kappa = 0.623$). The worst performing models overall were spectral class models developed using the data from the manned aircraft (RF $\kappa = 0.478$, LR $\kappa = 0.465$) followed by the models produced using the UAV-LS data. By contrast, the models developed using ALS data collected from a manned aircraft were the best performing models produced using data from this platform. The specificity for all classifiers was higher than the sensitivity. This is evidence that there were very few false negatives in the independent validation dataset but that a significant number of trees within the validation dataset were incorrectly classified (false negatives).

Table 4. Summary of the independent validation of model predictions. Model identifiers (Model ID) are as specified in Table 1.

Model ID	Platform	Class	Classifier	Kappa	Sensitivity	Specificity
5	Manned aircraft	Spectral	RF	0.4646	0.739	0.906
1	Manned aircraft	Spectral + ALS	RF	0.6023	0.802	0.994
3	Manned aircraft	ALS	RF	0.6086	0.803	1
5	Manned aircraft	Spectral	LR	0.4777	0.749	0.906
1	Manned aircraft	Spectral + ALS	LR	0.569	0.781	0.988
3	Manned aircraft	ALS	LR	0.6091	0.804	1
4	UAV	Spectral	RF	0.633	0.819	1
2	UAV	Spectral + UAV-LS	RF	0.6225	0.815	1
3	UAV	UAV-LS	RF	0.5044	0.778	1
4	UAV	Spectral	LR	0.7089	0.865	1
2	UAV	Spectral + UAV-LS	LR	0.6073	0.802	1
3	UAV	UAV-LS	LR	0.4898	0.716	1

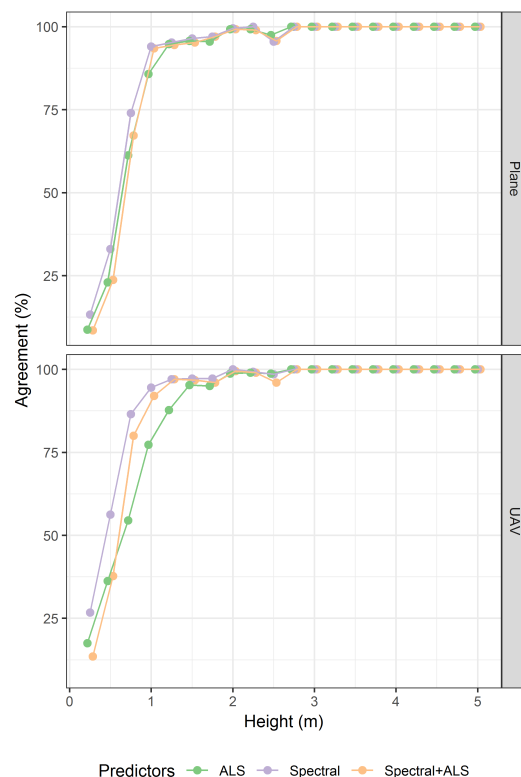


Figure 6. Agreement values for the independent validation dataset for trees within each height class. Each datum shows the mean of the agreement value for both the combined RF and LR models.

Sampling the field dataset as described above provided insight into the relationship between tree size and classification accuracy. This is important to define whether trees can be identified with

a high degree of accuracy prior to the onset of coning in this environment. Plotting the agreement between observed and predicted values for the validation dataset (Figure 6) revealed that the pattern of detection accuracy was similar for both aerial platforms examined. The accuracy of classifiers from both platforms was low for the smallest trees studied (<0.25 m) with agreement between observed and predicted below 20%. As tree height increased, the agreement increased rapidly with both platforms approaching 90% agreement for trees 1 m tall. Above this height threshold, detection accuracy reached a 100% agreement between observed and predicted values for the remainder of the validation data. The gradient of the increase in agreement in Figure 6 provides insight into the relative performance of models with different sets of predictors. For classifiers based on data collected from the manned aircraft there was very little difference in the validation curves for the two classifiers examined, indicating that the specificity of these models was similar within a tree size class. By contrast, there was some differentiation in detection accuracy for the different models developed from the UAV data. The classifier developed using only UAV laser scanning was the worst performing model and the classifier did not reach 100% agreement between observed and predicted until trees with a height of 2 m were used for validation. The models developed with the UAV spectral data showed a steeper validation curve and approached almost perfect agreement when the trees in the validation dataset were 1 m tall.

4. Discussions

The results of this study clearly show that remotely sensed data collected from both a manned aircraft and a UAV platform can accurately detect invasive exotic conifers in a study site that was dominated by grassland and small shrub vegetation. The classification accuracy achieved in this study was greater than that reported in previous work aimed at detecting invasive conifers in New Zealand using combinations of ALS and multispectral data [22] or conventional airborne imagery [31]. This result was expected as the vegetation and terrain structure in this study were less complex than in the previous work, and spatial resolution of the remotely sensed datasets was higher [22]. In contrast to a previous invasive conifer detection study in a similar environment using conventional airborne imagery [31] we were able to identify much smaller trees including the vast majority of trees that had begun coning. This result is significant for managers seeking to eliminate infestations before they reach maturity and become seed sources and suggests that data with higher spectral and spatial resolution data is important for this purpose.

The classification accuracy achieved in this study was slightly higher than that reported in comparable supervised image classification approaches. For example, research from South Africa using UAV imagery for invasive plant detection in a semi-arid environment with relatively simple vegetation structure [51] reported kappa values of 0.8305 and 0.8088 using two different supervised classifiers. However, a conventional consumer grade RGB camera was used in this study and it is possible that the improved classification accuracy we obtained was due to the use of a narrow band multispectral sensor used. In more complex environments in Northern Portugal, UAV data has been found to yield lower kappa values (0.51) although these results may not compared directly because the target plant was not flowering in this study and the imagery used was of a coarser resolution [75].

Our results provide further evidence for the capability of combining multispectral imagery with ALS for detection of exotic conifers in concordance with previous studies [22,46]. We found that combining these two data sources led to the development of models with the highest classification accuracy. However, in contrast to the previous work, we did not find that the inclusion of ALS data added significantly to the classification accuracy levels. This is probably due to the ease of separating the target trees with the surrounding vegetation based on spectral properties in the study environment. This finding would likely be different in a site with greater vegetation height and more complex composition where the fusion of structural (ALS or UAV-LS) and spectral data would be critical. In more complex settings alternative approaches based on object-based image analysis or deep learning may be necessary to achieve the required accuracy levels.

This study has shown for the first time that UAV data can be used for highly accurate detection of the early stages of exotic conifer invasions that are characterized by very scattered individuals of smaller stature. This includes very small trees that may not yet have begun coning and provides an operational tool that supports the early and effective control of invasions before new seed dispersal can occur. Our results showed that only 0.07% of coning trees were shorter than the height threshold (1 m) where we could confidently detect invasive conifers at the cusp of spreading further with a very high degree of accuracy. These results offer the first development of methods for early detection of conifer invasions as there was previously no research into this topic in the existing literature [79].

The field dataset collected in this study represents the most detailed “ground-truth” dataset of its type to the best of our knowledge. This was the result of a significant amount of data collection effort by the field team. While detailed datasets can be collected for scientific purposes, such ground assessments would not be feasible for operational purposes including control and management planning. These applications require quantitative information such as coning state, species, tree density etc. Even simplified sampling of invasions is often seen as too costly and remotely sensed data and its analysis can provide such vital information more efficiently for operational tree invasion management across larger landscapes. The magnitude of this work effort shows the importance of developing suitable remote sensing methods for invasive conifer detection and monitoring. Remotely sensed data will be a vital tool for those responsible for control of invasive conifers and monitoring the efficacy of control efforts. These methods can potentially provide accurate information over larger areas using only limited financial resources. The comparison of data collected with different properties and different platforms in this study will also assist land managers with data collection options. The choice of platform and sensor used in practice will be influenced by the properties of the area of interest, the size of area for which information is required, and the budget for data collection. However, our results show that data collected from both UAV and manned aircraft provide viable and accurate methods for invasive conifer detection.

To the best of our knowledge this is the first study that directly compares UAV data to manned aircraft for invasive conifer detection with the intention of identifying trees before the onset of coning. Differences in the properties of the training datasets for each platform were observed. The lower quartile of the elevation distribution extracted from the UAV-LS data (Figure 4) was considerably lower for the manned aircraft dataset than for the UAV data. This may be the result of larger footprint and the resulting lower CHM resolution of the manned aircraft data compared to the UAV-LS dataset. Alternatively, this could be caused by the multiple, rather than single, return capability of the manned aircraft scanner resulting in a greater penetration and characterization of smaller trees and areas where the invasive conifer canopy was dense. Alternatively, the positional accuracy of the UAV-LS data cannot be ruled out as a source of this result despite the rigorous approach taken to minimize this error. Despite these differences data from both the UAV and the manned aircraft platforms resulted in high classification accuracy in this study.

Separate training datasets were developed for each data collection platform based on the remote sensing data. This was necessary because of the differences between the datasets due to the spectral properties, spatial resolution, and differences in shadow levels due to the time of year that the imagery had been acquired. The properties of the dataset showed better spectral separation between the invasive conifers and the surrounding tussock in the manned aircraft data. This may be the result of the greater sophistication of the manned aircraft mounted camera and the generally better illumination of the scene in the airplane imagery as it was collected in summer. Both data sources exhibited excellent differentiation in the elevations extracted from the ALS data. This is likely the result of the simplistic nature of the study site where most of the vegetation with a height significantly greater than zero were invasive conifers. The misclassification of objects below 1 m for ALS alone was due to tall tussocks and shrubs that were occasionally present at the site due to the land use history and effects of grazing on the surrounding vegetation.

Two different image classification approaches were successfully developed and compared for both data sources. The RF algorithm was carefully tuned using an exhaustive search, this requires significant additional computing time. The simpler LR classifier does not require tuning in the same manner and so is substantially less computationally demanding. The accuracy of both classifiers was very high and were comparable. The RF algorithm performed slightly better than LR for the more complex models including more predictors. However, for the simpler models containing fewer predictors the LR outperformed RF algorithm. As a result, in this study area we would recommend the use of the simpler algorithm as gains associated with the use of the machine learning were absent or minimal and do not justify the additional complexity of using a model of this type. However, this may not be the case in more complex environments where the ability of the machine learning algorithm to better characterize complex and non-linear patterns in the fitting data may be more valuable. Other research into image classification for invasive plant detection has used “one class” algorithms with the results suggesting a high level of accuracy [29,30]. These approaches have the advantage of only requiring identification of a single positive class during algorithm training. This means that errors associated with incorrectly specified training datasets would be reduced and the requirement for field data collection is lessened.

The performance of models with different candidate predictor variables provided insight into their capacity for invasive conifer detection. A particularly noteworthy observation was that there was little improvement in classification accuracy when ALS or UAV-LS data was combined with multispectral imagery. This result is likely the consequence of the simplistic vegetation structure and composition in the study site. The dominant short tussock grasses and exotic grasses have very different spectral properties to the invasive conifers; this is particularly evident during the summer months when the grasses are commonly brown. This finding indicates that significant expense can be avoided by only collecting one type of remote sensing data. However, the ALS and multispectral data collected from a manned aircraft for this study were collected during the same mission so there is limited additional cost for the acquisition and no negative aspects as long as the acquisition settings are optimized for the most important dataset. Currently UAVs of the type used in this study are not capable of carrying two miniaturized sensors to collect data over a large area. Developments in UAV technology such as large fixed wing UAVs with alternative power sources will likely make this feasible in the near future. It should also be noted that there is an additional cost associated with data storage and processing when additional datasets are collected.

5. Conclusions

In this paper, we have evaluated the capability of pixel-based classification methods to identify invasive conifers in a vulnerable grassland environment. We found that high-resolution data collected using both UAV and manned aircraft was valuable for this task. Critically, the vast majority of seed-producing individuals were accurately identified even though they were very small. This was in part due to the very high spatial resolution of the data acquired. Both data sources and both classification approaches examined provided highly accurate classification results.

Author Contributions: Conceptualisation, J.P.D., M.S.W., J.M. and T.S.H.P.; methodology, J.P.D., M.S.W., J.M. and T.S.H.P.; software, J.P.D.; validation, G.D.P.; formal analysis, J.P.D.; resources, T.S.H.P.; data curation, J.P.D. and T.S.H.P.; writing—original draft preparation, J.P.D.; writing—review and editing, M.S., T.S.H.P., J.M. and G.D.P.; visualisation, J.P.D.; supervision, M.S.W., J.M., T.S.H.P.; project administration, T.S.H.P.; funding acquisition, T.S.H.P.

Funding: This research was funded as part of the Winning Against Wildings Project funded by the New Zealand Ministry for Business Innovation and Employment (Contract Number C09X1611) and the Forest Growers Levy Trust. Additional funding was also provided by the Ministry for Primary Industries post-graduate scholarship fund.

Acknowledgments: The authors are extremely grateful to the diligent and professional efforts of Matthew Scott, Dave Henley, and Don McConchie who completed field data collection. Robin Hartley and Ben Morrow of Scion are acknowledged for collection of all UAV data, and Andy Burrell of LandPro Ltd. for provision of aerial survey data.

Conflicts of Interest: The authors declare no conflict of interest.

References

1. Farjon, A. *A Natural History of Conifers*; Timber Press: Portland, OR, USA, 2008.
2. Dash, J.P.; Moore, J.R.; Lee, J.R.; Klápské, J.; Dungey, H.S. Stand density and genetic improvement have site-specific effects on the economic returns from *Pinus radiata* plantations. *For. Ecol. Manag.* **2019**, *446*, 80–92. [[CrossRef](#)]
3. Watt, M.S.; Kimberley, M.O.; Dash, J.P.; Harrison, D.; Monge, J.J.; Dowling, L. The economic impact of optimising final stand density for structural saw log production on the value of the New Zealand plantation estate. *For. Ecol. Manag.* **2017**, *406*, 361–369. [[CrossRef](#)]
4. Yao, R.T.; Scarpa, R.; Turner, J.A.; Barnard, T.D.; Rose, J.M.; Palma, J.H.N.; Harrison, D.R. Valuing biodiversity enhancement in New Zealand’s planted forests: Socioeconomic and spatial determinants of willingness-to-pay. *Ecol. Econ.* **2014**, *98*, 90–101. [[CrossRef](#)]
5. Brockerhoff, E.G.; Jactel, H.; Parrotta, J.A.; Quine, C.P.; Sayer, J. Plantation forests and biodiversity: Oxymoron or opportunity? *Biodivers. Conserv.* **2008**, *17*, 925–951. [[CrossRef](#)]
6. Stephens, S.S.; Wagner, M.R. Forest Plantations and Biodiversity: A Fresh Perspective. *J. For.* **2007**, *105*, 307–313. [[CrossRef](#)]
7. Winjum, J.K.; Schroeder, P.E. Forest plantations of the world: Their extent, ecological attributes, and carbon storage. *Agric. For. Meteorol.* **1997**, *84*, 153–167. [[CrossRef](#)]
8. Van Minnen, J.G.; Strengers, B.J.; Eickhout, B.; Swart, R.J.; Leemans, R. Quantifying the effectiveness of climate change mitigation through forest plantations and carbon sequestration with an integrated land-use model. *Carbon Balance Manag.* **2008**, *3*, 3. [[CrossRef](#)] [[PubMed](#)]
9. Payn, T.; Carnus, J.M.; Freer-Smith, P.; Kimberley, M.; Kollert, W.; Liu, S.; Orazio, C.; Rodriguez, L.; Silva, L.N.; Wingfield, M.J. Changes in planted forests and future global implications. *For. Ecol. Manag.* **2015**, *352*, 57–67. [[CrossRef](#)]
10. Richardson, D.M.; Hui, C.; Nuñez, M.A.; Pauchard, A. Tree invasions: Patterns, processes, challenges and opportunities. *Biol. Invasions* **2014**, *16*, 473–481. [[CrossRef](#)]
11. Nuñez, M.A.; Chiuffo, M.C.; Torres, A.; Paul, T.; Dimarco, R.D.; Raal, P.; Policelli, N.; Moyano, J.; García, R.A.; Wilgen, B.W.V.; et al. Ecology and management of invasive Pinaceae around the world: Progress and challenges. *Biol. Invasions* **2017**, *19*, 3099–3120. [[CrossRef](#)]
12. Dainese, M.; Aikio, S.; Hulme, P.E.; Bertolli, A.; Prosser, F.; Marini, L. Human disturbance and upward expansion of plants in a warming climate. *Nat. Clim. Chang.* **2017**, *7*, 577–580. [[CrossRef](#)]
13. Rejmánek, M. Invasive trees and shrubs: Where do they come from and what we should expect in the future? *Biol. Invasions* **2014**, *16*, 483–498. [[CrossRef](#)]
14. Richardson, D.M.; Rejmánek, M. Trees and shrubs as invasive alien species—A global review. *Divers. Distrib.* **2011**, *17*, 788–809. [[CrossRef](#)]
15. Rejmánek, M.; Richardson, D.M. Trees and shrubs as invasive alien species—2013 update of the global database. *Divers. Distrib.* **2013**, *19*, 1093–1094. [[CrossRef](#)]
16. NZFOA. *New Zealand Plantation Forest Industry Facts and Figures*; Technical Report; New Zealand Forest Owners Association: Wellington, New Zealand, 2016.
17. Ledgard, N.J. Wilding conifers—New Zealand history and research background. In *Managing Wilding Conifers in New Zealand: Present and Future*; Hill, R., Zydenbos, S., Bezar, C., Eds.; New Zealand Plant Protection Society Inc.: Christchurch, New Zealand, 2003.
18. Peltzer, D.A. Ecology and consequences of invasion by non-native (wilding) conifers in New Zealand. *J. N. Z. Grassl.* **2018**, *80*, 39–46.
19. Howell, C.J.; McAlpine, K.G. Native plant species richness in non-native *Pinus contorta* forest. *N. Z. J. Ecol.* **2016**, *40*, 131–136. [[CrossRef](#)]
20. Ledgard, N. Wilding control guidelines for farmers and land managers. *N. Z. Plant Prot.* **2009**, *62*, 380–386.
21. Anon. *The Right Tree in the Right Place—New Zealand Wilding Conifer Management Strategy 2015–2030*; Ministry for Primary Industries: Wellington, New Zealand, 2011.
22. Dash, J.P.; Pearse, G.D.; Watt, M.S.; Paul, T. Combining Airborne Laser Scanning and Aerial Imagery Enhances Echo Classification for Invasive Conifer Detection. *Remote Sens.* **2017**, *9*, 156. [[CrossRef](#)]
23. Andrew, M.E.; Ustin, S.L. The role of environmental context in mapping invasive plants with hyperspectral image data. *Remote Sens. Environ.* **2008**, *112*, 4301–4317. [[CrossRef](#)]

24. Woods, D. The highs and lows of wilding conifer control operations: The good, the bad and the ugly! In *Managing Wilding Conifers in New Zealand—Present and Future, Proceedings of the NZ Plant Protection Society Workshop, Christchurch, New Zealand, 11 August 2003*; Hill, R.I., Zydenbos, S.M., Bezar, C.M., Eds.; NZPPS: Auckland, New Zealand, 2003; pp. 55–63; ISBN 0-478-10842-7.
25. Cochrane, P.; Grove, P. *Exotic Wilding Conifer Spread within Defined Areas of Canterbury High Country*; Environment Canterbury: Christchurch, New Zealand, 2013.
26. Hestir, E.L.; Khanna, S.; Andrew, M.E.; Santos, M.J.; Viers, J.H.; Greenberg, J.A.; Rajapakse, S.S.; Ustin, S.L. Identification of invasive vegetation using hyperspectral remote sensing in the California Delta ecosystem. *Remote Sens. Environ.* **2008**, *112*, 4034–4047. [[CrossRef](#)]
27. Hall, S.J.; Asner, G.P. Biological invasion alters regional nitrogen-oxide emissions from tropical rainforests. *Glob. Chang. Biol.* **2007**, *13*, 2143–2160. [[CrossRef](#)]
28. Underwood, E.; Ustin, S.; DiPietro, D. Mapping nonnative plants using hyperspectral imagery. *Remote Sens. Environ.* **2003**, *86*, 150–161. [[CrossRef](#)]
29. Piironen, R.; Fassnacht, F.E.; Heiskanen, J.; Maeda, E.; Mack, B.; Pellikka, P. Invasive tree species detection in the Eastern Arc Mountains biodiversity hotspot using one class classification. *Remote Sens. Environ.* **2018**, *218*, 119–131. [[CrossRef](#)]
30. Lopatin, J.; Dolos, K.; Kattenborn, T.; Fassnacht, F.E. How canopy shadow affects invasive plant species classification in high spatial resolution remote sensing. *Remote Sens. Ecol. Conserv.* **2019**. [[CrossRef](#)]
31. Sprague, R.; Godsoe, W.; Hulme, P.E. Assessing the utility of aerial imagery to quantify the density, age structure and spatial pattern of alien conifer invasions. *Biol. Invasions* **2019**. [[CrossRef](#)]
32. Næsset, E.; Nelson, R. Using airborne laser scanning to monitor tree migration in the boreal—Alpine transition zone. *Remote Sens. Environ.* **2007**, *110*, 357–369. [[CrossRef](#)]
33. Stumberg, N.; Ørka, H.O.; Bollandsås, O.M.; Gobakken, T.; Næsset, E. Classifying tree and nontree echoes from airborne laser scanning in the forest—Tundra ecotone. *Can. J. Remote Sens.* **2013**, *38*, 655–666. [[CrossRef](#)]
34. Hantson, W.; Kooistra, L.; Slim, P.A. Mapping invasive woody species in coastal dunes in the Netherlands: a remote sensing approach using LiDAR and high-resolution aerial photographs. *Appl. Veg. Sci.* **2012**, *15*, 536–547. [[CrossRef](#)]
35. Rees, W.G. Characterisation of Arctic treelines by LiDAR and multispectral imagery. *Polar Rec.* **2007**, *43*, 345–352. [[CrossRef](#)]
36. Thieme, N.; Martin Bollandsås, O.; Gobakken, T.; Næsset, E. Detection of small single trees in the forest–tundra ecotone using height values from airborne laser scanning. *Can. J. Remote Sens.* **2011**, *37*, 264–274. [[CrossRef](#)]
37. Stumberg, N.; Bollandsås, O.M.; Gobakken, T.; Næsset, E. Automatic Detection of Small Single Trees in the Forest-Tundra Ecotone Using Airborne Laser Scanning. *Remote Sens.* **2014**, *6*, 10152–10170. [[CrossRef](#)]
38. Næsset, E. Influence of terrain model smoothing and flight and sensor configurations on detection of small pioneer trees in the boreal—Alpine transition zone utilizing height metrics derived from airborne scanning lasers. *Remote Sens. Environ.* **2009**, *113*, 2210–2223. [[CrossRef](#)]
39. Stumberg, N.; Hauglin, M.; Bollandsås, O.M.; Gobakken, T.; Næsset, E. Improving Classification of Airborne Laser Scanning Echoes in the Forest-Tundra Ecotone Using Geostatistical and Statistical Measures. *Remote Sens.* **2014**, *6*, 4582–4599. [[CrossRef](#)]
40. Zimmermann, H.; Von Wehrden, H.; Damascos, M.A.; Bran, D.; Welk, E.; Renison, D.; Hensen, I. Habitat invasion risk assessment based on Landsat 5 data, exemplified by the shrub Rosa rubiginosa in southern Argentina. *Austral Ecol.* **2011**, *36*, 870–880. [[CrossRef](#)]
41. Homer, C.G.; Aldridge, C.L.; Meyer, D.K.; Schell, S.J. Multi-scale remote sensing sagebrush characterization with regression trees over Wyoming, USA: Laying a foundation for monitoring. *Int. J. Appl. Earth Obs. Geoinf.* **2012**, *14*, 233–244. [[CrossRef](#)]
42. Singh, N.; Glenn, N.F. Multitemporal spectral analysis for cheatgrass (*Bromus tectorum*) classification. *Int. J. Remote Sens.* **2009**, *30*, 3441–3462. [[CrossRef](#)]
43. Pouteau, R.; Meyer, J.Y.; Stoll, B. A SVM-based model for predicting distribution of the invasive tree Miconia calvescens in tropical rainforests. *Ecol. Model.* **2011**, *222*, 2631–2641. [[CrossRef](#)]
44. Xu, C.; Morgenroth, J.; Manley, B. Integrating Data from Discrete Return Airborne LiDAR and Optical Sensors to Enhance the Accuracy of Forest Description: A Review. *Curr. For. Rep.* **2015**, *1*, 206–219. [[CrossRef](#)]

45. Barbosa, J.M.; Asner, G.P.; Hughes, R.F.; Johnson, M.T. Landscape-scale GPP and carbon density inform patterns and impacts of an invasive tree across wet forests of Hawaii. *Ecol. Appl.* **2017**, *27*, 403–415. [[CrossRef](#)]
46. Hauglin, M.; Ørka, H.O. Discriminating between Native Norway Spruce and Invasive Sitka Spruce—A Comparison of Multitemporal Landsat 8 Imagery, Aerial Images and Airborne Laser Scanner Data. *Remote Sens.* **2016**, *8*, 363. [[CrossRef](#)]
47. Ghulam, A.; Porton, I.; Freeman, K. Detecting subcanopy invasive plant species in tropical rainforest by integrating optical and microwave (InSAR/PoIInSAR) remote sensing data, and a decision tree algorithm. *ISPRS J. Photogramm. Remote Sens.* **2014**, *88*, 174–192. [[CrossRef](#)]
48. Alves Aguiar, D.; Adami, M.; Fernando Silva, W.; Friedrich Theodor Rudorff, B.; Pupin Mello, M.; dos Santos Vila da Silva, J. Modis time series to assess pasture land. In Proceedings of the 2010 IEEE International Geoscience and Remote Sensing Symposium, Honolulu, HI, USA, 25–30 July 2010; pp. 2123–2126. [[CrossRef](#)]
49. Kattenborn, T.; Lopatin, J.; Förster, M.; Braun, A.C.; Fassnacht, F.E. UAV data as alternative to field sampling to map woody invasive species based on combined Sentinel-1 and Sentinel-2 data. *Remote Sens. Environ.* **2019**, *227*, 61–73. [[CrossRef](#)]
50. Perroy, R.L.; Sullivan, T.; Stephenson, N. Assessing the impacts of canopy openness and flight parameters on detecting a sub-canopy tropical invasive plant using a small unmanned aerial system. *ISPRS J. Photogramm. Remote Sens.* **2017**, *125*, 174–183. [[CrossRef](#)]
51. Mafanya, M.; Tsele, P.; Botai, J.; Manyama, P.; Swart, B.; Monate, T. Evaluating pixel and object based image classification techniques for mapping plant invasions from UAV derived aerial imagery: Harrisia pomanensis as a case study. *ISPRS J. Photogramm. Remote Sens.* **2017**, *129*, 1–11. [[CrossRef](#)]
52. De Sá, N.C.; Castro, P.; Carvalho, S.; Marchante, E.; López-Núñez, F.A.; Marchante, H. Mapping the Flowering of an Invasive Plant Using Unmanned Aerial Vehicles: Is There Potential for Biocontrol Monitoring? *Front. Plant Sci.* **2018**, *9*. [[CrossRef](#)]
53. Schneider, L.C.; Fernando, D.N. An Untidy Cover: Invasion of Bracken Fern in the Shifting Cultivation Systems of Southern Yucatán, Mexico. *Biotropica* **2010**, *42*, 41–48. [[CrossRef](#)]
54. De Sá, N.C.; Carvalho, S.; Castro, P.; Marchante, E.; Marchante, H. Using Landsat Time Series to Understand How Management and Disturbances Influence the Expansion of an Invasive Tree. *IEEE J. Sel. Top. Appl. Earth Obs. Remote Sens.* **2017**, *10*, 3243–3253. [[CrossRef](#)]
55. Oliphant, A.J.; Wynne, R.H.; Zipper, C.E.; Ford, W.M.; Donovan, P.F.; Li, J. Autumn olive (*Elaeagnus umbellata*) presence and proliferation on former surface coal mines in Eastern USA. *Biol. Invasions* **2017**, *19*, 179–195. [[CrossRef](#)]
56. Lantz, N.J.; Wang, J. Object-based classification of Worldview-2 imagery for mapping invasive common reed, *Phragmites australis*. *Can. J. Remote Sens.* **2013**, *39*, 328–340. [[CrossRef](#)]
57. Khare, S.; Latifi, H.; Ghosh, S.K. Multi-scale assessment of invasive plant species diversity using Pléiades 1A, RapidEye and Landsat-8 data. *Geocarto Int.* **2017**, *33*, 681–698. [[CrossRef](#)]
58. Ng, W.T.; Rima, P.; Einzmann, K.; Immitzer, M.; Atzberger, C.; Eckert, S. Assessing the Potential of Sentinel-2 and Pléiades Data for the Detection of *Prosopis* and *Vachellia* spp. in Kenya. *Remote Sens.* **2017**, *9*, 74. [[CrossRef](#)]
59. Dronova, I.; Spotswood, E.N.; Suding, K.N. Opportunities and Constraints in Characterizing Landscape Distribution of an Invasive Grass from Very High Resolution Multi-Spectral Imagery. *Front. Plant Sci.* **2017**, *8*, 890. [[CrossRef](#)]
60. Bhattacharai, G.P.; Cronin, J.T. Hurricane Activity and the Large-Scale Pattern of Spread of an Invasive Plant Species. *PLoS ONE* **2014**, *9*, e98478. [[CrossRef](#)]
61. Mirik, M.; Chaudhuri, S.; Surber, B.; Ale, S.; James Ansley, R. Detection of two intermixed invasive woody species using color infrared aerial imagery and the support vector machine classifier. *J. Appl. Remote Sens.* **2013**, *7*, 073588. [[CrossRef](#)]
62. Skowronek, S.; Ewald, M.; Isermann, M.; Kerchove, R.V.D.; Lenoir, J.; Aerts, R.; Warrie, J.; Hattab, T.; Honnay, O.; Schmidlein, S.; et al. Mapping an invasive bryophyte species using hyperspectral remote sensing data. *Biol. Invasions* **2017**, *19*, 239–254. [[CrossRef](#)]
63. Skowronek, S.; Asner, G.P.; Feilhauer, H. Performance of one-class classifiers for invasive species mapping using airborne imaging spectroscopy. *Ecol. Inform.* **2017**, *37*, 66–76. [[CrossRef](#)]

64. Chance, C.M.; Coops, N.C.; Crosby, K.; Aven, N. Spectral Wavelength Selection and Detection of Two Invasive Plant Species in an Urban Area. *Can. J. Remote Sens.* **2016**, *42*, 27–40. [CrossRef]
65. Amaral, C.H.; Roberts, D.A.; Almeida, T.I.R.; Souza Filho, C.R. Mapping invasive species and spectral mixture relationships with neotropical woody formations in southeastern Brazil. *ISPRS J. Photogramm. Remote Sens.* **2015**, *108*, 80–93. [CrossRef]
66. Calviño-Cancela, M.; Méndez-Rial, R.; Reguera-Salgado, J.; Martín-Herrero, J. Alien Plant Monitoring with Ultralight Airborne Imaging Spectroscopy. *PLoS ONE* **2014**, *9*, e102381. [CrossRef]
67. Ishii, J.; Washitani, I. Early detection of the invasive alien plant Solidago altissima in moist tall grassland using hyperspectral imagery. *Int. J. Remote Sens.* **2013**, *34*, 5926–5936. [CrossRef]
68. Mirik, M.; Ansley, R.J.; Steddom, K.; Jones, D.C.; Rush, C.M.; Michels, G.J.; Elliott, N.C. Remote Distinction of A Noxious Weed (Musk Thistle: CarduusNutans) Using Airborne Hyperspectral Imagery and the Support Vector Machine Classifier. *Remote Sens.* **2013**, *5*, 612–630. [CrossRef]
69. Dash, J.P.; Watt, M.S.; Pearse, G.D.; Heaphy, M.; Dungey, H.S. Assessing very high resolution UAV imagery for monitoring forest health during a simulated disease outbreak. *ISPRS J. Photogramm. Remote Sens.* **2017**, *131*, 1–14. [CrossRef]
70. Dash, J.P.; Pearse, G.D.; Watt, M.S. UAV Multispectral Imagery Can Complement Satellite Data for Monitoring Forest Health. *Remote Sens.* **2018**, *10*, 1216. [CrossRef]
71. Heaphy, M.; Watt, M.S.; Dash, J.P.; Pearse, G.D. UAVs for data collection—Plugging the gap. *N. Z. J. For.* **2017**, *62*, 23–30.
72. Lishawa, S.C.; Carson, B.D.; Brandt, J.S.; Tallant, J.M.; Reo, N.J.; Albert, D.A.; Monks, A.M.; Lautenbach, J.M.; Clark, E. Mechanical Harvesting Effectively Controls Young Typha spp. Invasion and Unmanned Aerial Vehicle Data Enhances Post-treatment Monitoring. *Front. Plant Sci.* **2017**, *8*. [CrossRef]
73. Lehmann, J.R.K.; Prinz, T.; Ziller, S.R.; Thiele, J.; Heringer, G.; Meira-Neto, J.A.A.; Buttschardt, T.K. Open-Source Processing and Analysis of Aerial Imagery Acquired with a Low-Cost Unmanned Aerial System to Support Invasive Plant Management. *Front. Environ. Sci.* **2017**, *5*, 44. [CrossRef]
74. Dvořák, P.; Müllerová, J.; Bartaloš, T.; Brůna, J. Unmanned aerial vehicles for alien plant species detection and monitoring. *ISPRS Int. Arch. Photogramm. Remote Sens. Spat. Inf. Sci.* **2015**, *XL-1/W4*, 83–90. [CrossRef]
75. Alvarez-Taboada, F.; Paredes, C.; Julián-Pelaz, J. Mapping of the Invasive Species Hakea sericea Using Unmanned Aerial Vehicle (UAV) and WorldView-2 Imagery and an Object-Oriented Approach. *Remote Sens.* **2017**, *9*, 913. [CrossRef]
76. Martin, F.M.; Müllerová, J.; Borgniet, L.; Dommange, F.; Breton, V.; Evette, A. Using Single- and Multi-Date UAV and Satellite Imagery to Accurately Monitor Invasive Knotweed Species. *Remote Sens.* **2018**, *10*, 1662. [CrossRef]
77. Bryson, M.; Reid, A.; Ramos, F.; Sukkarieh, S. Airborne vision-based mapping and classification of large farmland environments. *J. Field Robot.* **2010**, *27*, 632–655. [CrossRef]
78. Vaz, A.S.; Alcaraz-Segura, D.; Campos, J.C.; Vicente, J.R.; Honrado, J.P. Managing plant invasions through the lens of remote sensing: A review of progress and the way forward. *Sci. Total Environ.* **2018**, *642*, 1328–1339. [CrossRef]
79. Juanes, F. Visual and acoustic sensors for early detection of biological invasions: Current uses and future potential. *J. Nat. Conserv.* **2018**, *42*, 7–11. [CrossRef]
80. Wong, T.T. Performance evaluation of classification algorithms by k-fold and leave-one-out cross validation. *Pattern Recognit.* **2015**, *48*, 2839–2846. [CrossRef]
81. Immitzer, M.; Vuolo, F.; Atzberger, C. First Experience with Sentinel-2 Data for Crop and Tree Species Classifications in Central Europe. *Remote Sens.* **2016**, *8*, 166. [CrossRef]
82. Roussel, J.R.; Auty, D. lidR: Airborne LiDAR Data Manipulation and Visualization for Forestry Applications, R package version 2.0.3. 2018. Available online: <https://CRAN.R-project.org/package=lidR> (accessed on 20 July 2019).
83. R Core Team. *R: A Language and Environment for Statistical Computing*; R Foundation for Statistical Computing: Vienna, Austria, 2018.
84. GDAL Development Team. *GDAL—Geospatial Data Abstraction Library, Version 2.02*; Open Source Geospatial Foundation: Beaverton, OR, USA, 2016.
85. Breiman, L. Random Forests. *Mach. Learn.* **2001**, *45*, 5–32. :1010933404324. [CrossRef]

86. Kuhn, M. Caret: Classification and Regression Training, R package version 6.0-84. 2018. Available online: <https://CRAN.R-project.org/package=caret> (accessed on 20 July 2019).
87. Wright, M.N.; Ziegler, A. Ranger: A Fast Implementation of Random Forests for High Dimensional Data in C++ and R. *J. Stat. Softw.* **2017**, *77*, 1–17. [[CrossRef](#)]
88. Cohen, J. A Coefficient of Agreement for Nominal Scales. *Educ. Psychol. Meas.* **1960**, *20*, 37–46. [[CrossRef](#)]



© 2019 by the authors. Licensee MDPI, Basel, Switzerland. This article is an open access article distributed under the terms and conditions of the Creative Commons Attribution (CC BY) license (<http://creativecommons.org/licenses/by/4.0/>).